A NUMERICAL ANALYISIS OF CHEMICAL EQUILIBRIUM HYPERSONIC AIR FLOWS

Mauricio A. Pinheiro Rosa
e-mail: pinheiro@ieav.cta.br
Instituto de Estudos Avançados - IEAv/CTA
Rod. dos Tamoios, Km 5,5
12.231-970 - São José dos Campos - SP, Brasil

Abstract. *Hypersonic flows are investigated using the explicit finite difference MacCormack's time marching technique. The complete Navier-Stokes equations are treated in a 2D cartesian geometry and the shock waves caused by solid step obstacles and viscous boundary layer on flat plates are examined. The results include pressure, temperature, density and velocity profiles at several system cross-sections as well as 2D contours for different Mach numbers. This work has the purposes of validating and presenting results of a chemical and thermodynamic equilibrium gas model applied to hypersonic flows over step obstacles and flat plate. The thermodynamic properties of high temperature air are calculated from polynomial correlations obtained in the literature. As part of the work, a comparison between calculation results of equilibrium chemically reacting and calorically perfect air flowfields has been performed.*

Keywords*: Hypersonic Flow, Chemical Equilibrium, Shock Wave, Step Obstacle, Numerical Simulation*

1. INTRODUCTION

By raising the temperature of the air above a certain value, molecular vibrational mode starts becoming important. By further increasing the air temperature, molecular dissociation as well as recombination reactions may also occur. For even higher temperatures, the process of atomic ionization may also take place. Each one of these processes has some impact on the properties of the air and, in this case, the air can no longer be treated simply as a calorically perfect gas. For instance, for air at 1 atm pressure, the O_2 and N_2 molecular vibrational energies start becoming significant above approximately 800 K, whereas chemical reactions start only at approximately 2500 K with the O_2 dissociation, which is accompanied by N_2 dissociation (above 4000 K) and several recombination reactions. At considerably higher temperature, approximately 9000 K, all the nitrogen and oxygen molecules have already dissociated and atomic ionization starts taking place so that we have a partially ionized plasma (O, O^+, N, N^+ and electrons). Also important to mention is that pressure affects the dissociation and ionization onset temperatures as well (Anderson, 1989).

In a previous work, Toro *et al*. (2005), supersonic and hypersonic flows over step obstacles and flat plates were analyzed considering the air as a calorically perfect gas using a Cartesian 2D, explicit finite difference MacCormack's time marching computer code. As it is known, such a gas model does not take into account the high temperature effects in the air described in the previous paragraph, which become important at temperatures found in hypersonic flows, i.e., for flow speeds higher than Mach 5, approximately. So, the flow model in this code has been improved so that now it accounts for gas dynamic high temperature effects in the air by considering it as a mixture of chemically reacting calorically perfect gases in local thermodynamic and chemical equilibrium conditions.

Therefore, the main objectives of this work are to present both the flow model implemented in the above-mentioned 2D code and also a few code calculation results, which show that the flow model is able to reproduce well the main features of 2D hypersonic flows. It is important to mention at this point that the subject of numerical inaccuracies present in the results, inherent of the adopted numerical method, although it is an important matter, is not a concern in the present work.

For these purposes, two simple hypersonic flow problems were considered: one is the flat plate problem, which here is treated in the same fashion as in Anderson (1995) and the other is a step obstacle problem. These problems were chosen due to the different nature of the shock waves that appear in these two geometries. In the former one, the flat plate, the shock wave is basically due to the formation of a boundary layer over the plate, *i.e*., viscous effects, such that the shock is oblique. In the latter, the step obstacle, a detached shock wave is formed due to the bluntness of the obstacle, and, differently from the flat plate case, the shock is almost normal in front of the obstacle.

There are several ways of introducing a thermodynamics and chemical equilibrium gas model in a computer code. One would be to implement explicitly the statistical thermodynamics equations; another would be to use high temperature air property tables along with "look-up table" procedures; and the other would be to implement polynomial correlations of air property tabulated data. In this work, the latter case has been adopted for being easy and convenient to apply within the framework of flowfield calculations, using the correlations obtained by Srinivasan *et al*. (1987). As

will be seen next, the chemical equilibrium gas mathematical model is basically the same as for the calorically perfect gas one except for the state equations. So, the 2D computer code has now the options to solve both calorically perfect and chemical equilibrium gas models. Although, the chemical equilibrium gas model implemented in the code is valid also for low air temperature, the calorically perfect gas model was kept in the code since it is a good assumption for many applications, fast running and can be used for the purpose of comparison. As will be shown later on in this work, this option should be used with care for supersonic flow applications since it can be very inaccurate at high Mach numbers.

2. MATHEMATICAL FLOW MODELS

For a 2D compressible flow, the complete Navier-Stokes' equations in the conservative form can be written as (Anderson (1995):

$$\frac{\partial U}{\partial t}+\frac{\partial F}{\partial x}+\frac{\partial G}{\partial y}=0 \tag{1}$$

where U , F and G are column vectors given by

$$U=\begin{bmatrix}\rho\\ \rho u\\ \rho v\\ E_t\end{bmatrix} \tag{2}$$

$$F=\begin{bmatrix}\rho u\\ \rho u^2+p-\tau_{xx}\\ \rho uv-\tau_{xy}\\ (E_t+p)u-u\tau_{xx}-v\tau_{xy}+q_x\end{bmatrix} \tag{3}$$

$$G=\begin{bmatrix}\rho v\\ \rho uv-\tau_{xy}\\ \rho v^2+p-\tau_{yy}\\ (E_t+p)v-u\tau_{xy}-v\tau_{yy}+q_y\end{bmatrix} \tag{4}$$

where E_t is the total energy, *i.e*., the sum of the kinetic energy plus the internal energy , e ,per unit volume, defined as:

$$E_t=\rho\left(e+\frac{V^2}{2}\right) \tag{5}$$

The normal and shear stress parameters, in terms of velocity gradients, are given as:

$$\tau_{xx}=\lambda(\nabla\cdot\mathbf{V})+2\mu\frac{\partial u}{\partial x} \tag{6}$$

$$\tau_{yy} = \lambda(\nabla \cdot \mathbf{V}) + 2\mu \frac{\partial v}{\partial y} \tag{7}$$

$$\tau_{xy} = \tau_{yx} = \mu\left(\frac{\partial u}{\partial y} + \frac{\partial v}{\partial x}\right) \tag{8}$$

The components of the heat flux vector appearing in Eqs. (3) and (4) are given below:

$$q_x = -k\frac{\partial T}{\partial x} \tag{9}$$

$$q_y = -k\frac{\partial T}{\partial y} \tag{10}$$

In the above equations the symbols retain the usual meaning, i.e., x and y are the Cartesian coordinate system, ρ is the fluid density, u and v are the x and y components of the velocity vector $\mathbf{V}$ ($|\mathrm{V}| = V = \sqrt{u^2 + v^2}$), p is the pressure, μ is the molecular viscosity, λ is the second coefficient of viscosity, τ_{ij} ($i,j=x,y$) are the stress tensor components, q_i ($i=x,y$) are the heat flux components, T is the temperature and k is the thermal conductivity.

The viscosity is evaluated through Sutherland's law:

$$\mu = \mu_0 \frac{T^{3/2}}{T + 110}$$

where μ_0 is a reference value at sea level. The thermal conductivity, k, is given by

$$k = \frac{\mu\, c_{p,0}}{\mathrm{Pr}_0}$$

In order to close the system of equations given above, two additional state equations are necessary and they depend on the gas model adopted for the air.

For the calorically perfect gas model, the equations are:

The perfect gas equation:

$$p = \rho R T \tag{11}$$

and the internal energy equation given by:

$$\boldsymbol{e} = \boldsymbol{c}_{v,0}\boldsymbol{T} \tag{12}$$

where $c_{v,0} = R/(\gamma - 1)$ and $c_{p,0} = \gamma c_{v,0}$ are the specific heats at constant volume and constant pressure, respectively, R is the air constant and γ is the air ratio of specific heats considering the air as calorically perfect gas and Pr_0 is the free stream Prandtl number.

The other model considers the air as a mixture of chemically reacting perfect gases in chemical and thermodynamic equilibrium conditions. As already mentioned, the Srinivasan's polynomial correlations are used here to express the pressure and temperature in terms of two other thermodynamic properties in order to close the model. That is

$$p = f_1(\rho, e) \tag{13}$$

$$T = f_2(p, \rho) \tag{14}$$

where f_1 and f_2 are functions which are obtained by curve fitting of tabulated statistical thermodynamics data.

As described in Srinivasan e*t al*. (1987), these correlations are improvements made in the widely known Tannehill and Mugge correlations (Tannehill and Mugge, 1974) for air at equilibrium conditions, mainly near the interfaces

between regions with different curve fittings. Also, they are said to be valid for the whole spectrum of temperatures up to 25,000 K.

3. COMPUTATIONAL DOMAINS AND BOUNDARY CONDITIONS

The body geometries and computational domains for the two problems studied in this work are shown in Fig.1. For both geometries the flow enters the domain from the left boundary and leaves at the right boundary so that the free stream boundary condition is always imposed on the left boundary and extrapolation condition is used on the right boundary. For both cases, the computational domain is always made big enough to impose free stream conditions on the upper boundary as well. In the Obstacle case, for the lower boundary, symmetry condition at the obstacle mid-plane (stagnation plane) is used, which reduces the calculations to a half of the domain, as shown in Fig. 1 b).

The boundary conditions on the flat plate and solid obstacle surfaces are the familiar no slip flow condition ($u = v = 0$) and either the uniform temperature or the adiabatic wall condition for the thermal boundary condition. Pressure at the domain boundaries is obtained by extrapolation of interior point values wherever necessary. The free stream conditions are usually used as the problem initial condition.

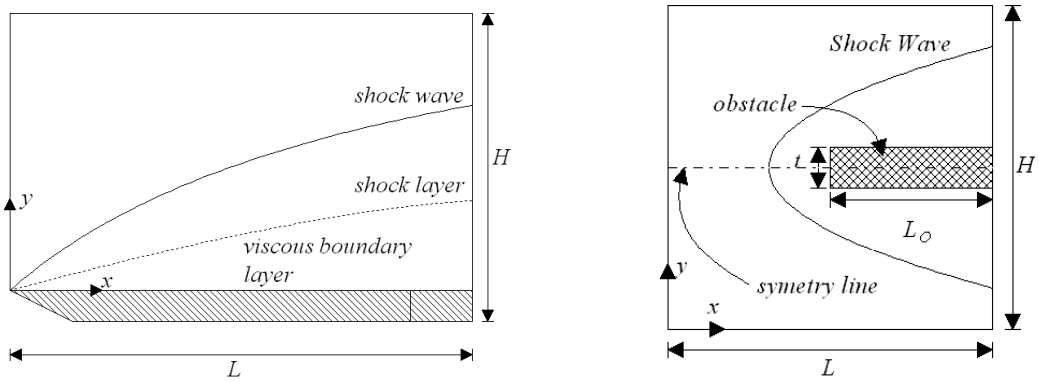

a) *b*)

Figure 1. Flat Plate and Flat Faced Obstacle Geometries.

4. NUMERICAL FRAMEWORK

As described in Toro *et al*. (2005), a computer code was developed to solve numerically, for the proposed problems, the mathematical model for calorically perfect gas using the shock capturing MacCormack's time marching scheme (Anderson (1995); (Hirsch, 1990). In this work, the proposed chemical equilibrium gas model has been incorporated to this computer code, so that now results for calorically perfect and chemical equilibrium gas models can be readily obtained and compared. The grids were generated using the LevSoft (1998) software.

Numerical subroutines for the Srinivasan's air property correlations for temperature and pressure have been implemented and validated separately by comparing their results with the ones in his original work (Srinivasan *et al*., 1987).

Also, a simple computer program that solves a system formed by conservation equations and additional state equations applied to a normal shock wave to calculate pressure, temperature, velocity, density and internal energy behind the shock wave for both, the calorically perfect gas model and the chemical equilibrium gas model using the Srinivasan's correlations, has been developed. For the calorically perfect gas case, the results are obtained from analytical solutions, whereas, for the equilibrium gas model, it solves a set of nonlinear equations using a numerical iterative procedure (Rosa, 2007). Since the models and methods in this code have been already verified and validated, its results will be used as part of the model and method validations in the 2D computer code.

5. ANALYSIS OF RESULTS

The free stream pressure ($\boldsymbol{p}_0$ = 101325 Pa), temperature ($\boldsymbol{T}_0$ =288.16 K) and density ($\boldsymbol{\rho}_0$ =1.225 kg/m^3), for all the cases analyzed, are those for the air at sea level. The free stream Mach number is giving by, $\mathbf{M} = \boldsymbol{u}_0 / \sqrt{\gamma \boldsymbol{R} \boldsymbol{T}_0}$, which

can be varied by changing the u_0 velocity value only. For the uniform wall temperature boundary condition cases, the free stream temperature value is used as the wall temperature. All results for the flow variables presented in this Section were normalized to the respective free stream values. The values of other parameters utilized in the calculations are given in Table **1**.

Table **1**. Parameter values considered in the calculations.

μ_0 (N·s/m^2)	Pr_0	R (kg/J·K)	γ
$1.458 \cdot 10^{-6}$	0.71	287.	1.4

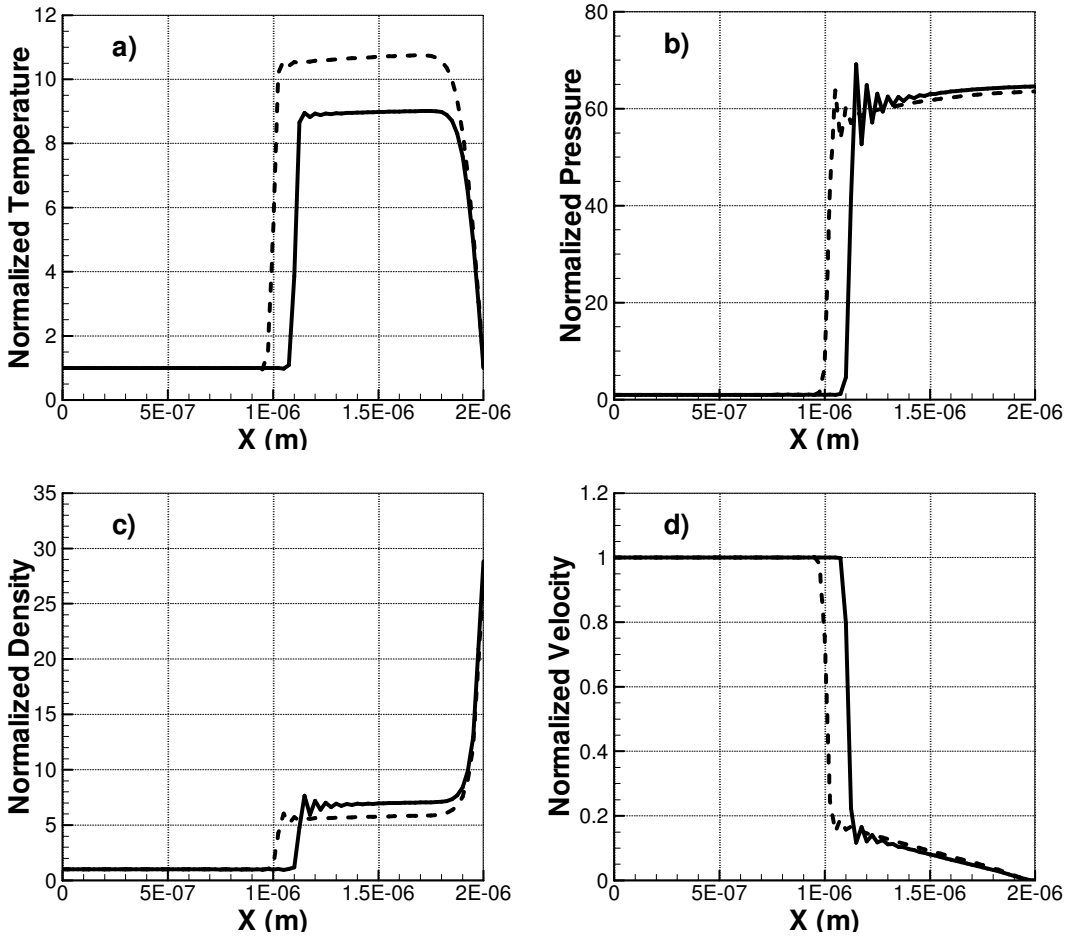

Figure 2. a) Temperature; b) Pressure; c) Density and d) Velocity profiles along the step obstacle's stagnation plane for calorically perfect gas (dashed line) and chemical equilibrium gas (solid line), for a Mach 7 free stream flow.

Figure 2 shows the steady-state temperature, pressure, density and velocity distributions along the stagnation (or symmetry) plane of a flat-faced obstacle, such as in Fig. 1, obtained with the 2D, finite-difference code for the calorically perfect and chemical equilibrium gas models. In these calculations it was considered a Mach 7 free stream flow and uniform temperature wall boundary condition. Firstly, it should be noticed that at the obstacle's stagnation plane, the shock wave is normal to the free stream, as can be seen schematically in Fig 1. At this point, it is important to mention that basically all the results presented in this work show that the MacCormack's algorithm, employed in the 2D code discussed here suffers of numerical dissipation (smear out flow discontinuities) as well as numerical dispersion (oscillations in front and behind of discontinuities). However, even with these drawbacks, this numerical scheme still yields satisfactory enough results to verify and validate the implementation of the chemical equilibrium gas model in the 2D code, as will be presented next. Of course, there are ways of improving the code results but this is not the objective in this work (see, for instance, Anderson (1995) and Hirsch (1990)).

Two important characteristics of the chemical equilibrium and calorically perfect gas model distributions at the stagnation plane are concerned with the behind the shock flow variable magnitudes and the shock layer thickness. As can be seen in Fig. 2, relative to the calorically perfect gas model results, the results behind the shock wave obtained with the chemical equilibrium gas model are only slightly higher for pressure, considerably lower for temperature and higher for density. Also shown in this figure, the higher density for the chemical equilibrium gas model has the effect of reducing the shock detachment distance (shock layer thickness) in front of the hypersonic flat-faced body. Also, can be seen in this figure that the temperature, pressure and density behind the shock wave continue to increase gradually toward the body face due to the continuous decrease in the flow velocity, which is stopped completely on the body surface. The density near the body face increases substantially because of the low free stream temperature boundary condition imposed on the solid surface. Figure 3.a) shows that the reduction in the shock layer thickness is not restricted only to the flow at stagnation plane but elsewhere in the calculation domain. The shock wave in a flat plate, shown in Figure 3.b), which is produced by the viscous boundary layer, is of the oblique type with a smaller wave angle for chemical equilibrium gas than that for a calorically perfect gas. All these observations are in agreement with the results of previous studies on high temperature effects on hypersonic flows found in the literature. Explanation in detail for these changes in the flow variable magnitudes behind the shock wave for the chemical equilibrium and perfect gas models can be found, for instance, in Anderson's book (Anderson, 1989). Here, it will only be said that since the temperature is a measure of the translational energy of the species, this will be higher for a calorically perfect gas because in this case the changes in kinetic energy across the shock is mostly converted to translational and rotational molecular energy modes behind the shock whereas, for a chemical equilibrium gas, this change in kinetic energy is shared among all molecular modes (translational, rotational, vibrational and electronic) and/or heats of formation of the chemical reaction products. For pressure, the relative change will be small because pressure behind the shock is mainly governed by the free stream velocity and thermodynamics effects are secondary.

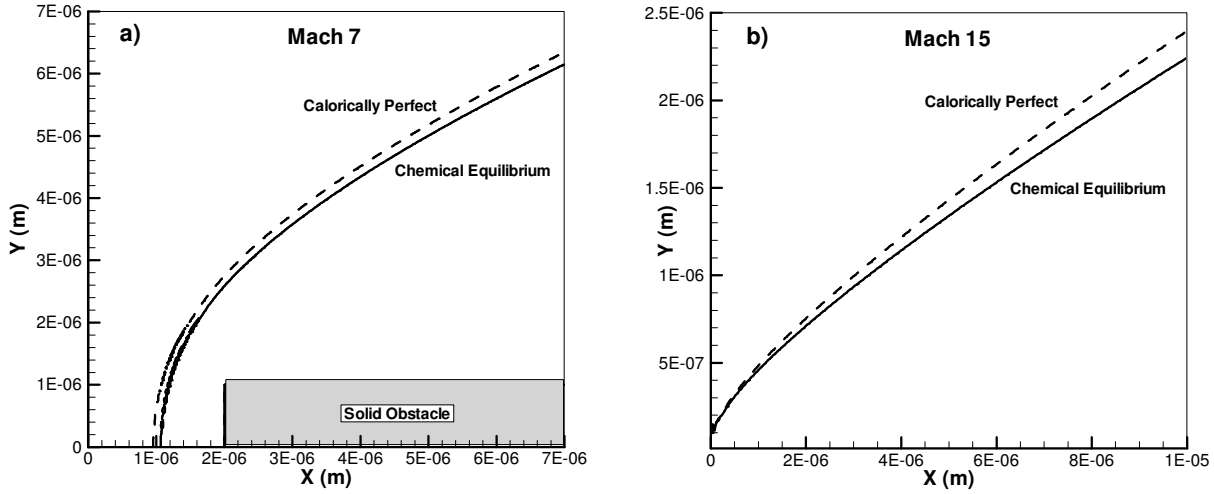

Figure 3. Shock wave front for calorically perfect and chemical equilibrium gas assumptions over: a) a step obstacle; b) a flat plate; for a Mach 7 and a Mach 15 free stream flow, respectively.

The analysis so far has shown that the chemical equilibrium gas model results obtained with the 2D computer code are qualitatively correct. So, next, the analysis will be concerned to show that the results are also quantitatively correct. Therefore, the behind the shock wave flow variable values, at the stagnation plane, will be compared with the respective ones obtained with the computer program that solves the normal shock wave model, described in the previous section. Figures 4 and 5 show the temperature, pressure, density and velocity distributions along the symmetry plane of a flat-faced obstacle obtained with the 2D, finite-difference, computer code. The results are for both calorically perfect and chemical equilibrium gas models, for three different free stream flow velocities (Mach 4, 7 and 10) and uniform wall temperature boundary condition. The behind the shock wave variable values can be inferred from these plots with a good accuracy if flow discontinuity smearing and oscillations produced by the numerical algorithm and also the fact that the variables do not remain exactly uniform behind the shock wave are taken into account. Therefore, the following procedure has been used: extrapolate the smooth part of the curve behind the shock (after the oscillations have vanished) towards the direction of the shock wave; draw a vertical line passing at the middle point between the starting and finishing (first oscillation) points of the shock sudden change; the behind the shock variable value estimate is given by the crossing point between these two lines. The results presented in Tables 2 and 3, for these inspected values, were obtained using this procedure by zooming the figures in order to get more accurate values. As can be noticed, the inferred values from the 2D, MacCormack's computer code calculations in Figures 4 and 5 are very close to the ones

calculated with the normal shock model program for both calorically perfect and chemical equilibrium gas models. So, all these results validate the models implemented in the 2D computer code.

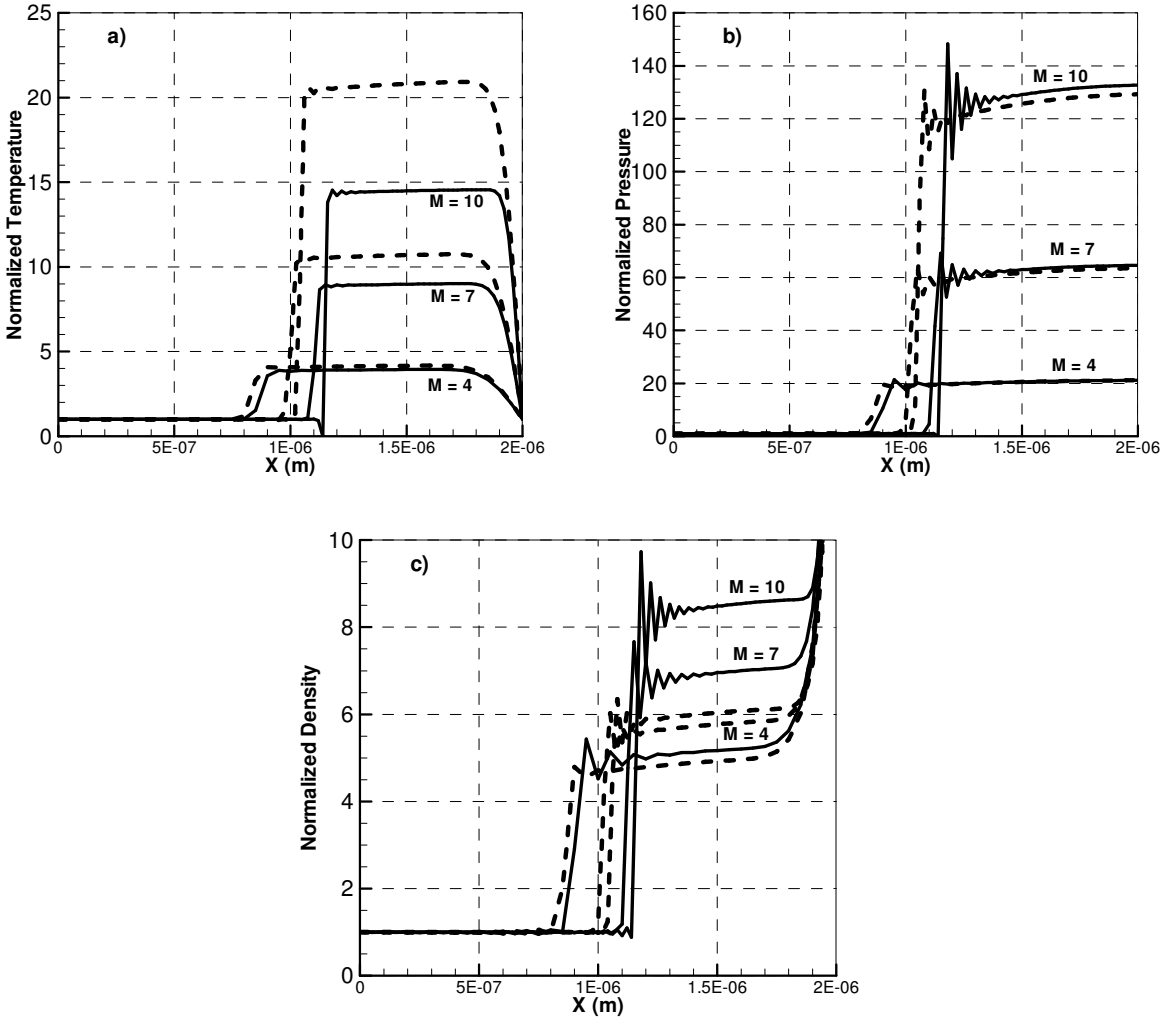

Figure 4. a) Temperature; b) Pressure and c) Density profiles along the step obstacle's stagnation plane for calorically perfect gas (dashed line) and chemical equilibrium gas (solid line), for Mach 4, 7 and 10 free stream flows.

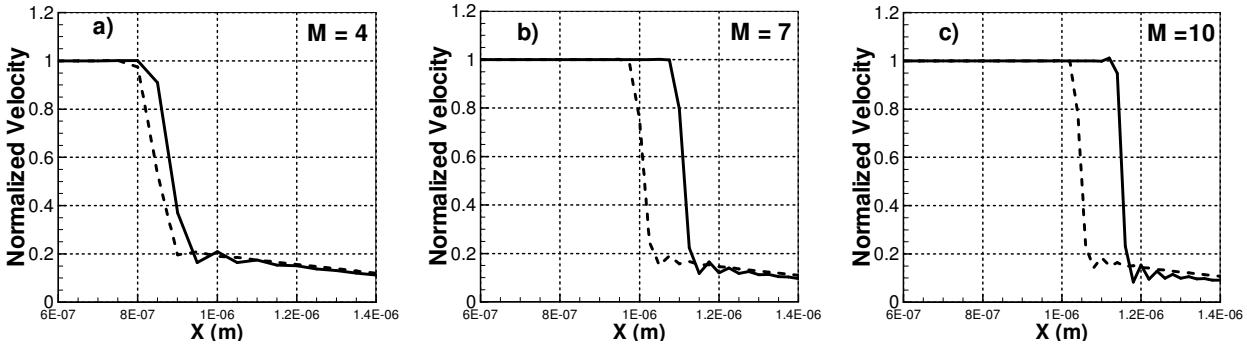

Figure 5. Velocity profiles along the step obstacle's stagnation plane for calorically perfect gas (dashed line) and chemical equilibrium gas (solid line), for a) Mach 4; b) Mach 7 and c) Mach 10 free stream flows.

Table 2. Behind the shock normalized flow variable results for the chemical equilibrium gas model.

	Chemical Equilibrium Gas Model					
	M = 4		**M = 7**		**M = 10**	
	(1)	**(2)**	**(1)**	**(2)**	**(1)**	**(2)**
Temperature	3.9	3.84	8.8	8.87	14.2	14.31
Pressure	19	18.78	60	59.26	124	124.09
Density	4.8	4.84	6.6	6.63	8.2	8.28
Velocity	0.21	0.207	0.14	0.151	0.12	0.13

(1) results obtained with the 2D computer code at the obstacle's stagnation plane.
(2) results obtained with the normal shock wave model computer code.

Table 3. Behind the shock normalized flow variable results for the calorically perfect gas model.

	Calorically Perfect Gas Model					
	M = 4		**M = 7**		**M = 10**	
	(1)	**(2)**	**(1)**	**(2)**	**(1)**	**(2)**
Temperature	4.2	4.05	10.4	10.47	20.3	20.39
Pressure	18.8	18.5	56	57.0	117	116.5
Density	4.6	4.57	5.5	5.44	5.7	5.71
Velocity	0.21	0.219	0.19	0.184	0.18	0.175

(1) results obtained with the 2D computer code at the obstacle's stagnation plane.
(2) results obtained with the normal shock wave model computer code.

In Fig. 4 and 5 can also be seen that the shock layer thickness reduces with increasing free stream Mach number (increasing density behind the shock). Since the calculated calorically perfect gas normalized density values tend towards a finite maximum value of about 6 for air as the free stream Mach number increases, the shock wave thickness tends towards a minimum. For the Mach 10 free stream, the shock layer thickness is already close to this minimum since the normalized density is about 5.7. Also, for the same free stream conditions, the chemical equilibrium gas shock layer is thinner than that for calorically perfect gas and is continually changing with increasing free stream Mach number. Table 4 presents the behind the shock parameter ratios of the chemical equilibrium to the calorically perfect gas model results for the three free stream Mach numbers. As can be noticed there, the high temperature effects on the flow variables become more pronounced with increasing flow free stream velocity, although, again, the pressure is the least affected.

Table 4. Behind the shock parameter ratios of the chemical equilibrium to the calorically perfect gas model results.

	M = 4	**M = 7**	**M = 10**
Temperature	0.95	0.85	0.70
Pressure	1.01	1.04	1.07
Density	1.06	1.22	1.45
Velocity	0.94	0.82	0.74

Figure 6 shows the temperature, pressure and density stagnation plane profiles for two distinct thermal boundary conditions at the solid wall: uniform wall temperature and adiabatic wall boundary conditions. As can be seen in these figures, the behind the shock wave variable values depend only on the free stream conditions, whereas near the solid face, the variables change according to the imposed wall boundary conditions. For the uniform free stream wall temperature boundary condition, the fast density growth near the wall is basically due to the fast temperature reduction there to meet the imposed wall value. On the other hand, for adiabatic wall boundary condition, since the temperature derivative should be zero at the wall, the flow variable changes near the wall are very small. Therefore, for the uniform wall temperature boundary case, the higher average density inside the shock yields a slightly thinner shock layer than the adiabatic case.

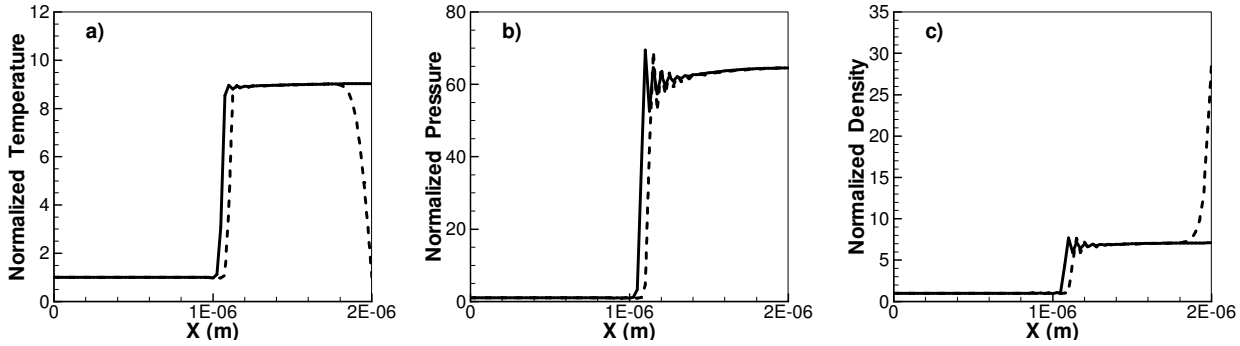

Figure 6. Step obstacle's stagnation plane a) temperature, b) pressure and c) density distributions for two distinct thermal boundary conditions on the obstacle: free stream uniform temperature (dashed line) and adiabatic wall (solid line).

Finally, Fig. 7 show the temperature contour maps for a Mach 7 free stream, considering the chemical equilibrium gas model, for the uniform wall temperature and adiabatic wall boundary conditions, calculated with the 2D computer code. As can be noticed in these figures, the difference between the maps is basically inside the thermal boundary layer on the front and side walls.

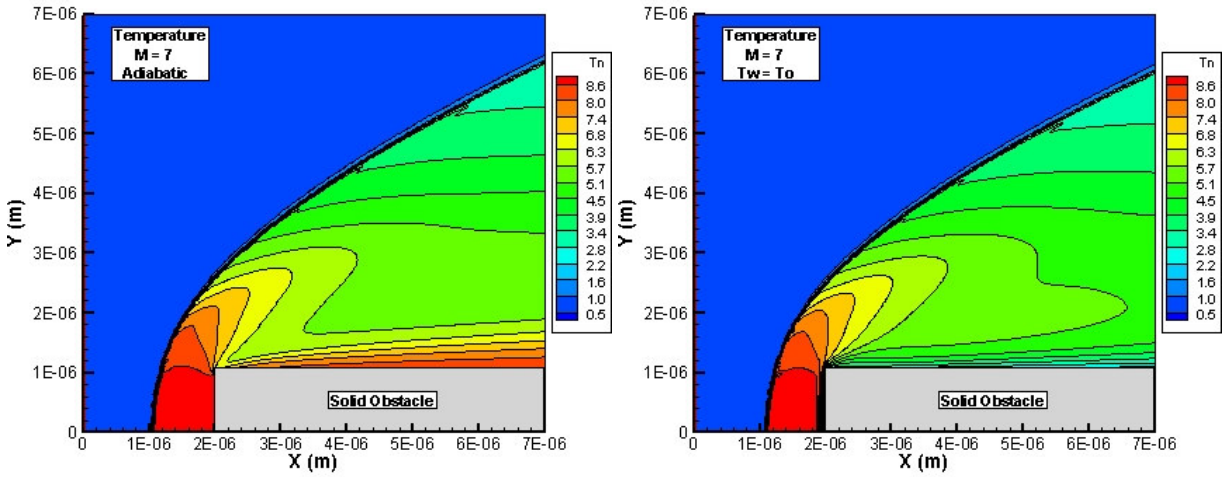

Figure 7. Mach 7 free stream temperature contours over a solid step obstacle for uniform temperature and adiabatic wall thermal boundary conditions.

6. COMMENTS AND CONCLUSIONS

Polynomial correlations for air temperature and pressure properties, which consider high temperatures effects assuming chemical and thermodynamic equilibrium conditions, have been tested separately and within of a 2D, finite-difference, framework. The results, in this work, have been used not only for code verification and gas model validations, which are the main objectives of this work, but also to show how high temperature affects the flow variables with normal and/or oblique shock waves. As could be observed, the calorically perfect gas model becomes very inaccurate for flow free stream velocities higher than Mach 6, approximately, and the use of a chemically reacting gas model is then a need. Also, the results in this work give confidence to use such gas models to study more complex hypersonic flows than the ones presented here.

It is important to comment also that although the assumption of chemical equilibrium is good enough for accurate analysis of various hypersonic flow applications, in a few others it is necessary to consider the mixture of gases in chemical non-equilibrium if accurate results are required. So, next improvements to the models presented herein will be to consider chemical non-equilibrium.

7. REFERENCES

Anderson, J. D. Jr., 1989, "Hypersonic and High Temperature Gas Dynamics", McGraw Hill, US.

Anderson, J. D. Jr., 1995, “Computational Fluid Dynamics”, McGraw Hill, New York.

Hirsch C., 1990, “Numerical Computation of Internal and External Flows: Computational Methods for Inviscid and Viscous Flows”, Vol. 2, John Wiley & Sons.

Rosa, M. A. P., 2007, “A Chemical Equilibrium Gas Model Normal Shock Wave Computer Program”, IEAv Report, to be published.

Srinivasan, S.; Tannehill J. C. and Weilmuenster K. J, 1987, “Simplified Curve Fits for the Thermodynamic Properties of Equilibrium Air”, NASA CR-1181.

Tannehill, J. C. and P. H. Mugge, 1974, “Improvement Curve Fits for the Thermodynamic Properties of Equilibrium Air Suitable for Numerical Computation Using Time-dependent or Shock Capturing Methods”, NASA CR-2470.

Toro, P. G. P.; Rocamora Jr., F. D.; Rosa, M. A. P.; Minucci, M. A. S., 2005, ”High Speed Flow Over a Flat Plate and Step Obstacle”, 18th International Congress of Mechanical Engineering, COBEM 2005, Ouro Preto, MG.

“LEVSOFT: A Software Platform for 2D Computer Aided Engineering”, 1998, http://www.lev.ieav.cta.br